Dynamics of water molecules in an alkaline environment

Dynamics of water molecules in an alkaline environment

Han-Kwang Nienhuys[a)]
FOM Institute for Atomic and Molecular Physics, Kruislaan 407, 1098 SJ Amsterdam, The Netherlands and Schuit Catalysis Institute, Eindhoven University of Technology, P.O. Box 513, 5600 MB Eindhoven, The Netherlands

Arjan J. Lock
FOM Institute for Atomic and Molecular Physics, Kruislaan 407, 1098 SJ Amsterdam, The Netherlands

Rutger A. van Santen
Schuit Catalysis Institute, Eindhoven University of Technology, P.O. Box 513, 5600 MB Eindhoven, The Netherlands

Huib J. Bakker[b)]
FOM Institute for Atomic and Molecular Physics, Kruislaan 407, 1098 SJ Amsterdam, The Netherlands and University of Amsterdam, Nieuwe Achtergracht 129, 1018 WS, Amsterdam, The Netherlands

(Received 27 November 2001; accepted 8 August 2002)

We report on a two-color mid-infrared pump–probe spectroscopic study of the dynamics of the OH stretch vibrations of HDO molecules dissolved in a concentrated (10 M) solution of NaOD in D_2O. We observe that spectral holes can be created in the broad OH stretch absorption band that change neither position nor width on a picosecond time scale. This behavior differs strongly from that of pure HDO:D_2O where rapid spectral diffusion ($\tau_c \approx 600$ fs) occurs. The long-living inhomogeneity indicates that a concentrated aqueous NaOX (X=H,D) solution has a very static hydrogen-bond network. The results also show that the absorption band of the OH stretch vibration consists of two separate classes of OH groups with very different vibrational lifetimes. For component I, the lifetime of the OH stretch vibration is ~600 fs and increases with OH frequency, which can be explained from the accompanying decrease in the strength of the hydrogen-bond interaction. This component represents HDO molecules of which the OH group is bonded to a D_2O molecule via a $DO–H\cdots OD_2$ hydrogen bond. For component II, the lifetime is ~160 fs, and does not show a significant frequency dependence. This component represents HDO molecules that are hydrogen bonded to a D_2O molecule or an OD^- ion. The short, frequency-independent vibrational lifetime of component II can be explained from the participation of the HDO molecule and its hydrogen-bonded partner in deuteron and/or proton-transfer processes. © *2002 American Institute of Physics.* [DOI: 10.1063/1.1510670]

I. INTRODUCTION

Dissolving a salt in water leads to a strong change of the viscosity of the liquid that is believed to result to a large extent from the ion-induced changes of the structure of the hydrogen-bond network that links the water molecules.[1–3] Recently, experiments showed that water molecules in the solvation shells of negative ions (e.g., Cl^-) behave very differently from those in bulk water.[4] For example, the hydrogen bond length $DO–H\cdots Cl^-$ varies on a much slower time scale (~12 ps) than the otherwise comparable hydrogen bond $DO–H\cdots OD_2$ between two water molecules (~500–700 fs[5,6]).

An interesting question is what happens if the negative ion is a base B^- that can accept protons or deuterons from neighboring water molecules according to

$$HO–H\cdots B^- \rightarrow HO^-\cdots H–B. \quad (1)$$

Even for a weak base, the hydrogen bond between water and the base ion is much stronger than that among water molecules or between water molecules and halide ions. As a result, the difference between the hydrogen bond and the covalent OH bond gets blurred. A special example of this blurring is when the left and right side of the reaction [Eq. (1)] are identical, which happens if the base is a hydroxyl (OH^-) ion.

Infrared spectroscopy forms an ideal method to study hydrogen-bond interactions, because the absorption frequency of an OH stretch vibration is strongly correlated to the length of the hydrogen bond between its H atom and a neighboring atom (usually O, N, or a negative ion). High and low OH stretch frequencies correspond to long (weak) and short (strong) hydrogen bonds, respectively. The highest OH stretch frequency occurs in the gas phase (about 3700 cm^{-1}); for extremely strong hydrogen bonds, the OH-stretch frequency can become as low as 800 cm^{-1} (Refs. 7–11).

Figure 1 shows infrared absorption spectra of OH groups in different environments. The dashed curve represents the spectrum of liquid D_2O with a small amount of D atoms substituted by H atoms, yielding an HDO in D_2O solution for

a)Current address: Department of Chemical Physics, Lund University, Box 124, SE-221 00 Lund, Sweden.
b)Electronic mail: h.bakker@amolf.nl

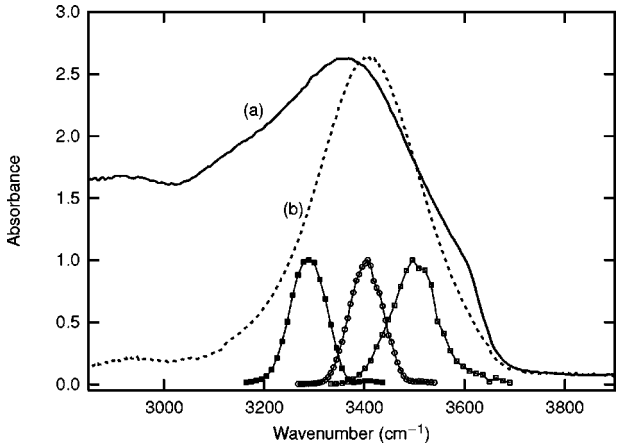

FIG. 1. Absorbance spectra of O–H groups in (a) HDO in D_2O and (b) 10 M NaOD in D_2O in which a small fraction of D atoms is substituted by H atoms (referred to as NaOX solution). A background of a pure (unsubstituted) sample was subtracted. The small curves on the bottom indicate the excitation spectra used in the experiments. The NaOX solution has a slightly larger concentration of H atoms than the HDO solution.

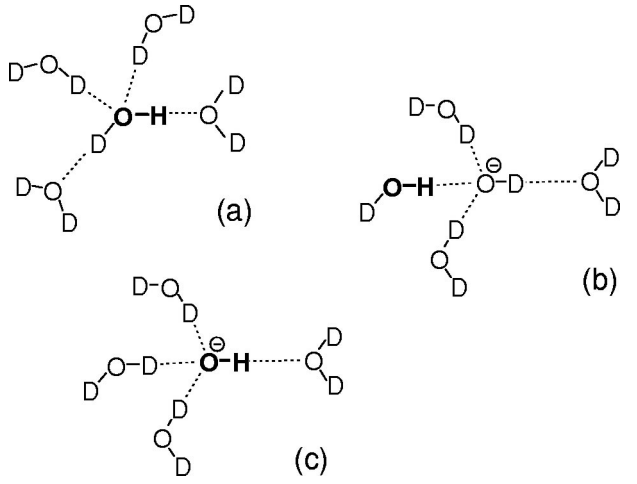

FIG. 2. Different classes of OH groups in the NaOX solution. (a) $DO–H\cdots OD_2$; (b) $DO–H\cdots OD^-$; (c) $DOD\cdots O–H^-$. These are limiting cases; in reality, there will be intermediate cases with a more delocalized charge.

which the OH stretch absorbance spectrum has a width of 270 cm^{-1} and a central frequency of 3405 cm^{-1}. The solid curve represents the spectrum of a protonated 10 mol/l NaOD in D_2O solution. In this case, a mixture containing OH groups both in OH^- ions and in HDO molecules is obtained (further denoted as ''NaOX solution''). The high concentration of OD^- ions has a remarkable effect on the OH stretch absorption band. The spectrum broadens strongly towards lower frequencies, and a shoulder appears around 3600 cm^{-1}.

The very broad absorbance spectrum of the NaOX solution is not understood in detail, but has been interpreted as follows.[12,13] The Na^+ ions have no direct effect on the OH stretch spectrum, because water molecules do not form hydrogen bonds with positive ions. In contrast, the OX^- (X =D,H) ions are embedded in the hydrogen-bond network, and the OH groups can have many possible configurations with respect to their direct environment. Roughly, we can distinguish three categories for these OH groups. In the range 3200–3500 cm^{-1}, we see the majority of HDO molecules, which donate hydrogen bonds to other HDO or D_2O molecules [as in Fig. 2(a)]. This is comparable to the situation of HDO dissolved in D_2O [Fig. 1(a)], except that the central frequency is shifted to a somewhat lower value. This means that hydrogen bonds are, on the average, shorter (and stronger) in the NaOX solution than in HDO:D_2O. This is not surprising, given the overall higher density of oxygen atoms at this NaOD concentration (62 mol/l, compared to 56 mol/l in plain water).

At lower frequencies, the absorption results from HDO molecules that form strong hydrogen bonds with OD^- ions [Fig. 2(b)]. Depending on the exact geometry and the relevant interactions, the complex may also be described as an $HD_4O_3^-$, $HD_6O_4^-$, or $HD_8O_5^-$ complex.[13–17] The OD^- ion can easily accept protons or deuterons from neighboring HDO or D_2O molecules.

Finally, the shoulder at 3600 cm^{-1} is attributed to the OH^- ions [Fig. 2(c)]. OH^- ions are only weak donors of hydrogen bonds due to their negative charge.[14] The resulting long and weak $OH^-\cdots OD_2$ hydrogen bonds[14,17] cause their frequency to be rather high.[12]

Up to now, most knowledge on the effect of OH^- ions in a liquid solution results from non-time-resolved experiments, such as infrared[13] and Raman[18] spectroscopy, dielectric relaxation,[19] and neutron diffraction.[20] Extensive data on the geometry and thermodynamic properties of the solvated OH^- ion are available from calculations (see, for example, Refs. 16, 17, 21, 22, and the references to experimental work therein). Direct information on the dynamics has only been provided by *ab initio* molecular-dynamics simulations. These simulations showed that the structure of the hydrogen-bond network and proton/deuteron transfer are strongly related,[14,23] and that the proton is delocalized in a $H_3O_2^-$ complex.[15]

In this paper, we present an experimental study of the microscopic structure and dynamics of water in a strongly alkaline solution with time-resolved mid-infrared spectroscopy. We found that this method provides much more information on the dynamics and structure of water molecules in a strongly alkaline environment than was obtained before with conventional spectroscopic techniques.

II. EXPERIMENT

In a mid-infrared pump–probe experiment, an intense infrared pulse (pump pulse) tuned to a specific frequency (ranging from 3030 to 3500 cm^{-1}) excites a significant fraction of the molecules from the vibrational ground ($v=0$) state to the excited ($v=1$) state. This causes a transient change in the absorbance spectrum: around the pump frequency, the absorbance decreases, whereas at lower frequencies, corresponding to the $v=1\rightarrow 2$ transition, the absorbance increases. This so-called transient spectrum is obtained by measuring the absorbance of an independently tunable probe pulse. After the excitation by the pump pulse, the transient spectrum will rapidly return to the thermal equilibrium spectrum. This relaxation process can be followed in time by

varying the time delay between pump and probe pulses, which thus provides information about the dynamics of the NaOX solution.

A. Infrared generation

To generate the infrared pump and probe pulses, we used a commercial titanium–sapphire amplifier (Quantronix Titan) that generates 3 mJ, 100 fs pulses at a wavelength of 805 nm and a repetition rate of 1 kHz. These near-infrared pulses were split into two separate branches; one, containing most of the pulse energy, for the pump pulse generation and one for the probe pulse generation. In each branch, part of the 805 nm pulse pumped an optical parametrical generation and amplification stage based on a β-barium borate (BBO) crystal (Light Conversion Topas). This stage generated pulses with a wavelength tuned in the range between 2100 and 2250 nm. In another BBO crystal, a second-harmonic-generation process converted these pulses to the range 1050–1125 nm, that were used as a seed for a parametric amplification process pumped by the remaining 805 nm light in a potassium titanyl phosphate (KTP) crystal. In the latter process, mid-infrared pulses are generated that are tunable in the range 2800–3450 nm (3600–2900 cm^{-1}) with a pulse duration of ~250 fs and a full width at half maximum (FWHM) of ~80–120 cm^{-1}. The pump pulse energy was typically 10–20 μJ, and the probe pulse energy was typically 1 μJ.

B. Sample

The sample consists of a 200 μm-thick layer of a 10 mol/l solution of NaOD in D_2O (a concentrated NaOD:D_2O solution was obtained from Sigma-Aldrich, which was appropriately diluted), in which a small amount of the deuterium atoms was replaced by hydrogen atoms, such that the transmission of this sample in the range 2900–3600 cm^{-1} was approximately 4%, corresponding to a D:H ratio of about 100:1. The sample is held in between two 4 mm-thick calcium fluoride windows.

The sample was at room temperature and at a fixed position in the laser beam focus, which leads to some heating of the sample. By numerically solving the heat diffusion equation in the sample and sample windows, we estimate that the maximum temperature increase was 11 K (for 20 μJ pump pulses in a focus with a 100 μm diameter). All results presented in this paper are, therefore, for a temperature $T = 303 \pm 6$ K.

C. Pump–probe setup

The pump–probe setup is a slightly adapted version of the one described in Ref. 24. Here, we use separate CaF_2 lenses to focus the pump and probe pulses into a ~100 μm diameter spot in the sample. A half-wave plate rotates the probe pulse polarization to the magic angle (54.7 degrees) with respect to the pump pulse polarization, in order to be insensitive to the reorientation of the excited molecules.[24] With a chopper, every other pump pulse is blocked, which enables the measurement of the absorbance change $\Delta\alpha \equiv -\ln(T(t)/T_0)$, where t is the time delay between the pump and probe pulses, $T(t)$ is the corresponding transmission of the probe, and T_0 is the reference transmission of the probe pulse, without the effect of a pump pulse. In each measurement, we measured the absorbance change $\Delta\alpha(t)$ for a large number of delay values t, while we kept the pump and probe frequencies (ω_{pu} and ω_{pr}, respectively) fixed. This procedure was repeated for a number of pump and probe frequencies, which thus yields a three-dimensional data set $\Delta\alpha(\omega_{pu}, \omega_{pr}, t)$.

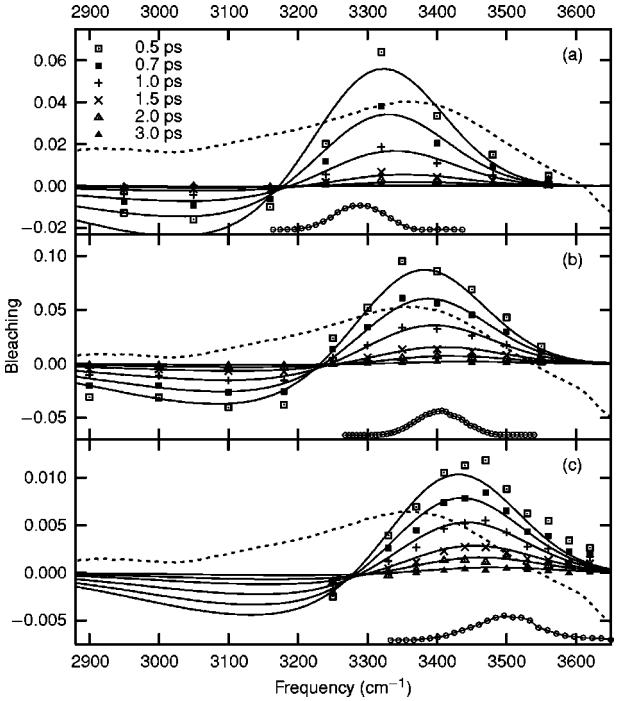

FIG. 3. Transient spectra of the NaOX solution (data points) at several different pump–probe delays, for excitation at (a) 3290, (b) 3405, and (c) 3500 cm^{-1}. The bleaching is defined as $-\Delta\alpha = \ln(T/T_0)$. The data points at the bottom of each plot indicate the pump pulse spectra. The drawn curves result from Eq. (8) with the parameters from Table I and the dashed curves represent the linear absorbance spectrum (see also Fig. 1), that is much broader than the bleaching bands.

III. RESULTS

A. Transient spectra

By combining experimental data for different probe frequencies, we constructed transient spectra of the NaOX solution for excitation at pump frequencies $\omega_{pu} = 3290$, 3405, and 3500 cm^{-1}. Figure 3 shows these transient spectra for delays $t \geqslant 0.5$ ps. From these spectra it follows that the OH absorption band of the NaOX solution is strongly inhomogeneous: The bleaching signals are much narrower than the linear absorbance spectrum and the frequency of the maximum bleaching signal depends strongly on the pump frequency, even at larger delay times ($\geqslant 2$ ps). This means that the excitation leads to the formation of a spectral hole that persists on a picosecond time scale. This is in contrast to the situation in HDO:D_2O,[5,6,25,26] where the bleaching rapidly acquires the shape of the linear absorbance spectrum.

The spectral holes shown in Fig. 3 have a full width at half maximum (FWHM) of approximately 200 cm^{-1} and are much broader than the convoluted spectrum of the pump and probe pulses. This implies that the OH stretch absorption

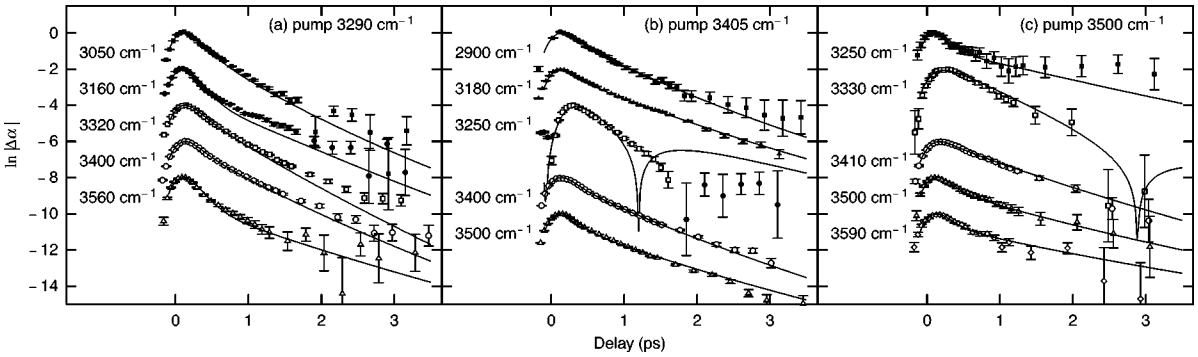

FIG. 4. Pump–probe scans on the NaOX solution for different pump and probe pulse frequencies (data points). The data are plotted logarithmically as $\ln|\Delta\alpha|$. Data points with open symbols correspond to bleaching ($\Delta\alpha<0$); filled symbols correspond to induced absorbance ($\Delta\alpha>0$). To aid comparison, the curves and data points are shifted vertically—the true amplitudes can be read from Fig. 3. The curves result from Eq. (8) with parameters from Table I. The two curves with singularities are explained in the last paragraph of Sec. III D.

band of the NaOX solution is not purely inhomogeneously broadened, but also contains a broadening contribution of a fast spectral modulation process. The characteristic time scale of this fast spectral modulation process is on the order of a few hundred femtoseconds, because the shapes of the spectral holes only show changes at delays <0.5 ps.

Figure 4 shows typical pump–probe delay scans at various $(\omega_{pu},\omega_{pr})$ combinations. At delays >0.5 ps, the experimental data show a more rapid decay for lower probe frequencies than for higher frequencies, in both the bleaching band and the induced-absorbance band. This observation shows that the vibrational lifetime T_1 of the OH stretch vibration depends on frequency. Indeed, it has been found before that the value of T_1 decreases with decreasing OH stretch frequency, as a result of the accompanying increase of the strength of the OH$\cdots$O hydrogen-bond interaction.[27,28]

B. Dynamics at small delays

Most of the pump–probe delay scans shown in Fig. 4 deviate strongly from single-exponential decays and decay significantly faster at small delays than at large delays. This fast initial decay is also visible for high pump and probe frequencies, which implies that it cannot be explained from the increase of T_1 with OH frequency. One might think that the fast initial decay results from the same fast spectral modulation process that leads to the large width of the spectral holes shown in Fig. 3. The presence of a fast spectral modulation process implies that a relatively narrow bleaching band should appear in the transient spectrum that directly after excitation broadens and decreases in amplitude. Therefore, for equal pump and probe frequencies, the spectral modulation would cause an initial rapid decay of the absorbance change, since this decay results from both the spectral diffusion and the vibrational relaxation. For pump and probe frequencies that differ, the initial decay would be slower, because then the molecules would diffuse into the spectral window of the probe leading to a (partial) compensation of the decay caused by vibrational relaxation. However, the fast initial decay is also observed in data sets where the pump and probe frequencies differ. Hence, the initial decay cannot be the result of spectral modulation, but instead likely represents an independent absorbance component of the OH stretch absorbance band with a very short vibrational lifetime. The time constant of the fast initial component (further denoted as component II) is $\sim$160 femtoseconds, which means that it is approximately four times faster than the decay of the slow component (further denoted as component I).

C. Modeling of the transient spectra and delay scans

The spectral hole burning results of Fig. 3 show that the OH absorption band of the NaOX solution is strongly inhomogeneously broadened, but also contains a line broadening contribution due to a fast spectral modulation process. The line shape resulting from the fast spectral modulation process can be described with a Gauss–Markov model or with an overdamped Brownian oscillator[29] model. These models both describe the spectral diffusion as a stochastic modulation of the transition frequency ω within a Gaussian spectral distribution $f_B(\omega)$ with central frequency ω_B and standard deviation Δ_B.

$$f_B(\omega)\propto\exp(-(\omega-\omega_B)/2\Delta_B^2), \tag{2}$$

The rate of the stochastic modulation is characterized with a time constant τ_c for the exponential decay of the autocorrelation function of the detuning from the central frequency ω_B

$$\langle(\omega(t)-\omega_B)(\omega(0)-\omega_B)\rangle=\Delta_B^2 e^{-t/\tau_c}, \tag{3}$$

With increasing value of τ_c, the shape of the spectral response changes from a Lorentzian (homogeneous limit, $\Delta_B\tau_c\ll1$) to a Gaussian (inhomogeneous limit, $\Delta_B\tau_c\gg1$).

In our experiments, only a small spectral diffusion effect at short delays is observed, which indicates that τ_c is on the order of the pulse duration, i.e., $\sim$200 femtoseconds. From the width of the spectral holes of Fig. 3 it follows that the standard deviation Δ_B of the Gaussian distribution of the fast modulation process is $\sim$65 cm^{-1}. Hence, $\Delta_B\tau_c\approx2.5$ (note that 1 cm^{-1} is 0.18 ps^{-1}), which implies that the fast spectral modulation process is in the inhomogeneous limit. This means that the spectral response of the fast modulation process should have a (nearly) Gaussian shape, which agrees well with the observed shape of the spectral holes.

The transient spectra and transient delay scans as measured in a two-color pump–probe experiment depend not only on the shape of the linear $0\rightarrow1$ absorption, but also on

the spectra of the $1\rightarrow0$ stimulated emission, the $1\rightarrow2$ excited-state absorption, and the pump and probe pulse properties. All these effects on the shape of the transient spectra can be accounted for in an analytic description of the Brownian oscillator in the overdamped and inhomogeneous limit $(\Delta_B\tau_c\gg1)$.[5,29]

In the Brownian oscillator model, spectral diffusion results from diffusion in a harmonic potential (''Brownian oscillation'') of a low-frequency coordinate. In this case, the low-frequency coordinate is the hydrogen-bond length R, i.e., the O–H$\cdots$O length. The fact that the excitation frequency of the OH group depends roughly linearly on R (Refs. 7 and 8) implies that the hydrogen-bond potential of the excited state ($v=1$) has its minimum at a different value of R [see Fig. 5(a)]. After the excited population has equilibrated within the $v=1$ potential, the $v=1\rightarrow0$ stimulated emission contribution to the pump–probe signal is centered at a frequency $\omega_B-\delta\omega_{sto}$, where $\delta\omega_{sto}$ is the Stokes shift [Fig. 5(c)]. This Stokes shift and the standard deviation Δ_B have the relation

$$\delta\omega_{sto}=\hbar\Delta_B^2/k_BT, \tag{4}$$

where $\hbar$ is Planck's constant divided by 2π and k_B is Boltzmann's constant.

In the limit that: (a) The Brownian oscillator is overdamped, (b) the stochastic modulation is in the inhomogeneous limit, and (c) the time t is larger than the correlation time τ_c, a relatively simple expression for the transient spectral response is obtained

$$B(\omega_B,\omega_{pu},\omega_{pr})=Ae^{-t/T_1(\omega_B)}[B_{01}+B_{10}-\sigma B_{12}], \tag{5}$$

with components

$$A=\frac{1}{D}\exp(-(\omega_{pu}-\omega_B)^2/2(\Delta_B^2-\Delta_{pu}^2)), \tag{6a}$$

$$B_{01}=\exp(-[\omega_{pr}-\omega_{01}]^2/2D^2), \tag{6b}$$

$$B_{10}=\exp(-[\omega_{pr}-\omega_{10}]^2/2D^2), \tag{6c}$$

$$B_{12}=\exp(-[\omega_{pr}-\omega_{12}]^2/2a^2D^2). \tag{6d}$$

$$D^2=\Delta_B^2+\Delta_{pr}^2, \tag{6e}$$

with $\omega_{01}=\omega_B$, $\omega_{10}=\omega_B-\delta\omega_{sto}$, and $\omega_{12}=\omega_B-\delta\omega_{anh}$, where $\delta\omega_{anh}$ is the anharmonic shift of the OH stretch vibration. In this expression it is assumed that the pump and probe pulse spectra are Gaussians with central frequencies ω_{pu} and ω_{pr} and standard deviations Δ_{pu} and Δ_{pr}, respectively. The total signal has an amplitude A that is determined by the efficiency of the excitation by the pump pulse. The terms B_{ij} represent the contributions to the signal for the $v=i\rightarrow j$ transitions. The Gaussian contributions B_{01} and B_{10} have identical standard deviations D, and B_{12} has a standard deviation aD, where a is a scaling factor (see Fig. 5). Figure 5(b) shows the (qualitative) behavior of the components B_{ij}. The quantity σ is the relative cross section of the $v=1\rightarrow2$ transition as compared to the $v=0\rightarrow1$ transition.

The term $e^{-t/T_1(\omega_B)}$ represents the frequency-dependent vibrational lifetime of the OH stretch vibration. This dependence on the OH stretch frequency ω_B can be described as

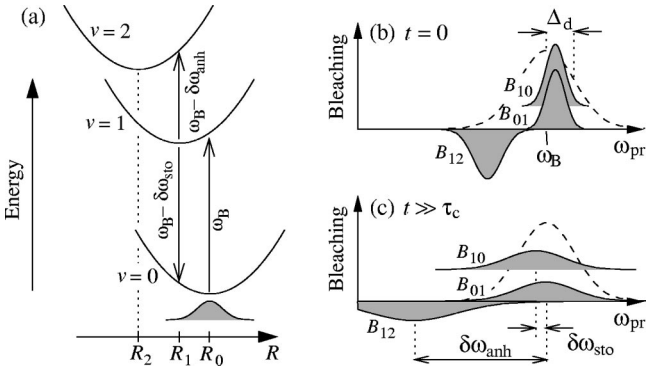

FIG. 5. In (a), schematic potentials of the Brownian oscillator model, for a single central frequency ω_B are shown. The potential energy is a function of the hydrogen bond length R for every state v of the OH stretch vibration and is approximated by a parabolic potential. The central frequency for a thermal population (shaded area) in the ground-state potential is ω_B. For a thermal population at the bottom of the $v=1$ potential, the $v=1\rightarrow0$ transition frequency has a Stokes shift $\delta\omega_{sto}$ and the $v=1\rightarrow2$ transition frequency has an anharmonic redshift $\delta\omega_{anh}$. The relative position of the $v=2$ potential is defined by $a=(R_2-R_1)/(R_1-R_0)$. In (b) and (c), the contributions B_{ij} to the transient spectrum [Eq. (5)] are shown schematically, for a pump frequency slightly larger than ω_B. The dashed line indicates the linear absorbance spectrum.

$$T_1(\omega_B)=\tau_{OH}(1-\omega_B/\omega_{gas})^{-1.8}, \tag{7}$$

where $\omega_{gas}=3707\ cm^{-1}$ is the frequency of the OH stretch vibration in gas-phase HDO,[30] and τ_{OH} is a constant. This relation results from quantum-mechanical calculations on the coupling between the hydrogen bond and the OH stretch vibration,[31] and was verified for a wide range of hydrogen-bonded complexes[27] and for HDO molecules dissolved in D_2O.[28]

From the results of Fig. 3, it follows that the OH stretch absorption band has persistent inhomogeneous character. Hence, to describe the total transient spectral response, the response of a single Brownian oscillator should be convoluted with an inhomogeneous distribution function. In addition, the presence of two independent absorbance components with different vibrational lifetimes should be accounted for. Each of these components is thus modeled as a Gaussian inhomogeneous distribution of Brownian oscillators

$$S(\omega_{pu},\omega_{pr},t)=\int d\omega_B[c_If_{I,i}(\omega_B)B_I(\omega_B,\omega_{pu},\omega_{pr},t)+c_{II}f_{II,i}(\omega_B)B_{II}(\omega_B,\omega_{pu},\omega_{pr},t)], \tag{8}$$

where I and II denote the two absorbing components and $f_{x,i}$ (with $x=$I,II) the inhomogeneous distribution function of each of the two components. Since we do not have any *a priori* information on the exact composition of the linear absorption spectrum of the NaOX solution in Fig. 1, we take $f_{x,i}$ to be Gaussian

$$f_{x,i}(\omega_B)=\exp(-(\omega_B-\omega_{x,0})^2/2\Delta_{x,i}^2),(x=\text{I,II}). \tag{9}$$

We find that Eq. (8), convoluted with the pump–probe pulse cross correlate, provides a very good description of the experimental data of Figs. 3 and 4. The parameter values that result from a fit of these results are shown in Table I.

TABLE I. Model parameters [Eqs. (2)–(9)] for the NaOX solution. Sec. III D describes how these parameter values are obtained.

Parameter		Value
Component I central frequency	$\omega_{\mathrm{I},0}$	3336 cm^{-1}
Bandwidth Brownian oscillator[a]	$\Delta_{\mathrm{I,B}}$	65 cm^{-1}
Inhomogeneous bandwidth[a]	$\Delta_{\mathrm{I,i}}$	78 cm^{-1}
Anharmonic redshift	$\delta\omega_{\mathrm{I,anh}}$	284 cm^{-1}
Stokes shift	$\delta\omega_{\mathrm{I,sto}}$	20 cm^{-1}
Scaling factor for displacement $v=2$	a_{I}	2.6
$v=1\rightarrow 2$ relative cross section	σ_{I}	1.5
Vibrational lifetime prefactor $[T_{\mathrm{I},1}(\omega_{\mathrm{B}})=\tau_{\mathrm{OH}}(1-\omega_{\mathrm{B}}/\omega_{\mathrm{gas}})^{-1.8}]$	τ_{OH}	6.7 fs
Component II central frequency	$\omega_{\mathrm{II},0}$	3429 cm^{-1}
Bandwidth Brownian oscillator[a]	$\Delta_{\mathrm{II,B}}$	81 cm^{-1}
Inhomogeneous bandwidth[a]	$\Delta_{\mathrm{II,i}}$	115 cm^{-1}
Anharmonic redshift	$\delta\omega_{\mathrm{II,anh}}$	245 cm^{-1}
Stokes shift	$\delta\omega_{\mathrm{II,sto}}$	32 cm^{-1}
Scaling factor for displacement $v=2$	a_{II}	0.7
$v=1\rightarrow 2$ relative cross section	σ_{II}	1.6
Vibrational lifetime	$T_{\mathrm{II},1}$	0.16 ps

[a]Bandwidths refer to standard deviations of Gaussian line shapes. To obtain the FWHM, multiply by 2.35.

D. Fit procedure and results

For delays $t\geqslant 0.5$ ps, the shape of the transient spectra and transients is nearly entirely determined by component I, with parameters $\omega_{\mathrm{I},0}$, $\Delta_{\mathrm{I,B}}$, $\Delta_{\mathrm{I,i}}$, $\delta\omega_{\mathrm{I,anh}}$, α_{I}, and τ_{OH}. The Stokes shift $\delta\omega_{\mathrm{I,sto}}$ follows from $\Delta_{\mathrm{I,B}}$ [Eq. (4)]. Hence, these parameters are determined by a simultaneous least-squares fit on the transient spectra at a large number of delays $t\geqslant 0.5$ ps. Subsequently, we use these fit results in a fit of the transients as a function of delay time (as in Fig. 4), to determine $\omega_{\mathrm{II},0}$, $\Delta_{\mathrm{II,B}}$, $\Delta_{\mathrm{II,i}}$, $\delta\omega_{\mathrm{II,anh}}$, α_{II}, $T_{\mathrm{II},1}$, c_{I}, and c_{II}.

The formal errors in the parameters in the fits were fairly small (typically a fraction 10^{-3} of the parameter value). However, the model assumes that the pulse spectra, pulse time envelopes, and inhomogeneous and diffusive bandwidths all have ideal Gaussian shapes. The fact that the true shapes are not Gaussian is most likely a more significant, but very difficult to calculate, source of errors. Therefore, we do not show the formal errors, because these are not representative of the true uncertainties.

From the parameter values shown in Table I it is clear that the two absorbance components mainly differ in their vibrational lifetime. Component II has an extremely short decay constant $T_{\mathrm{II},1}$ of $\sim$160 fs that is independent of the pump and probe frequencies within our experimental accuracy. In contrast, the vibrational lifetime of component I does strongly depend on frequency. This frequency dependence is well accounted for by Eq. (7). Due to this frequency dependence, the transient spectra shift slightly towards higher frequencies with increasing delay, because the lower-frequency parts of both the bleaching bands and the induced-absorbance bands decay slightly faster than their higher-frequency counterparts. This also means that the frequency with zero absorbance change shifts towards higher frequencies. This effect causes the singularities in the (logarithmically plotted) curves for $\omega_{\mathrm{pr}}=3250\ \mathrm{cm}^{-1}$ in Fig. 4(b) and $\omega_{\mathrm{pr}}=3330\ \mathrm{cm}^{-1}$ in Fig. 4(c), which show a transition from bleaching to induced absorbance. The delay value at which the bleaching and induced absorbance at a particular frequency compensate each other is extremely sensitive to the exact line shapes of the $v=0\rightarrow 1$ and $v=1\rightarrow 2$ contributions, which explains why the singularity in the experimental data and the model are at somewhat different time delays.

IV. DISCUSSION

In plain HDO:D_2O, spectral diffusion covers the entire OH stretch absorption band of the linear spectrum, with a correlation time of $\sim$600 fs. Such a type of spectral diffusion is completely absent for the NaOX solution, for which the absorption spectrum is inhomogeneously broadened on at least a picosecond time scale. This means that the hydrogen-bond network, which determines the spectral broadening of the OH stretch vibration, is immobilized by the presence of a high concentration of Na^+ and OX^- ions. Neutron diffraction experiments[20] recently showed that the O–O radial distribution function, which is related to the structure of the NaOX solution, is indeed very different from that of water. Apparently, the disturbed structure of the hydrogen-bond network allows only for small rapid fluctuations, leading to a nearly instantaneous broadening of the spectral holes. The NaOX solution has a high density of the NaOX solution (62 M O atoms) with respect to plain water (56 M O atoms). However, this high density is not likely the direct cause of the slow hydrogen-bond dynamics; from the compressibility $\kappa=45\times 10^{-6}\ \mathrm{bar}^{-1}$ (Ref. 32) of water, we estimate that water reaches a 62 M O-atom density at a pressure of 2.6 kbar. From the neutron diffraction data,[20] the equivalent pressure was estimated to be even higher, i.e., 9 kbar. However, the reorientation time of water, that is closely related to the hydrogen-bond dynamics (changing the orientation of a water molecule requires stretching and/or breaking its hydrogen bond[24]), changes by only $\sim$17% going from ambient pressure to 4 kbar, or by 20% at 9 kbar.[33] This small effect of the density is confirmed by the behavior of the viscosity. The viscosity of water, also related to the making and breaking of

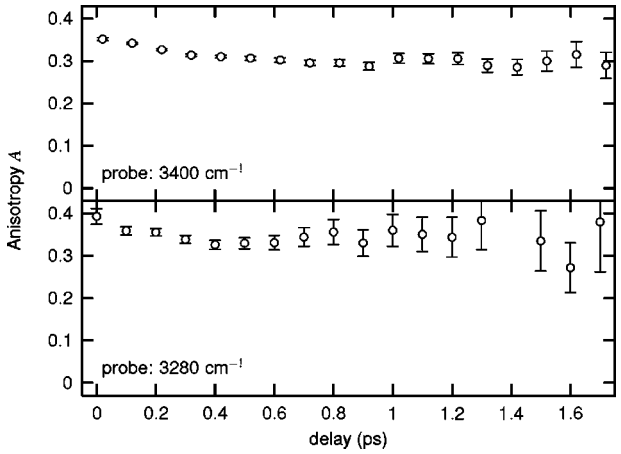

FIG. 6. Rotational anisotropy of a 10 M NaOX mixture pumped at 3400 cm^{-1} as a function of delay. Only at small delays, a small decay of the anisotropy is observed, for longer delays the anisotropy stays nearly constant.

hydrogen bonds, increases by only 20% and 80% for 4 and 9 kbar, respectively.[33] In contrast, the viscosity of a 10 M NaOH solution is a factor 13.5 larger than the viscosity of pure water.[32] These considerations suggest that high charge density, rather than high particle density, is responsible for the absence of subpicosecond hydrogen-bond dynamics for a concentrated aqueous solution of NaOD.

Additional support for the observed absence of hydrogen-bond dynamics is provided by data on the reorientation of OH groups in the NaOX mixture. We performed polarization resolved measurements similar to the pump–probe delay scans of Fig. 4 on a 10 M NaOX solution, where we excited with a pump frequency of 3400 cm^{-1} and measured the absorbance change $\Delta\alpha(t)$ separately for parallel ($\parallel$) and perpendicular ($\perp$) probe polarizations.[24] From these data, we calculated the rotational anisotropy

$$R(t)=\frac{\Delta\alpha_{\parallel}(t)-\Delta\alpha_{\perp}(t)}{\Delta\alpha_{\parallel}(t)+2\Delta\alpha_{\perp}(t)}. \tag{10}$$

The pump pulse preferentially excites OH groups that are approximately parallel to the polarization of the pump pulse, such that $R=0.4$ at $t=0$. The decay of R indicates to what extent the OH groups can change reorientation; free orientational motion would result in $R\rightarrow 0$. Figure 6 shows the decay of the anisotropy for probe frequencies centered at 3400 and 3280 cm^{-1}. Clearly, the decay of the anisotropy is limited to a small decrease at delays $t\lesssim 0.5$ ps, which indicates that each individual OH group can only change its orientation within a limited angular range. This result strongly differs from that of similar experiments on HDO dissolved in D_2O,[24] where the anisotropy decays with a time constant of 2.7 ps. The observed limited decay of the anisotropy is in agreement with the observed absence of hydrogen-bond dynamics, since large changes in the orientation of an OH group must involve stretching, making, and/or breaking of hydrogen bonds. We can, therefore, regard the structure of the hydrogen-bond network as a ''gel''-like state.

The broadening due to the small and rapid fluctuations in the immobilized hydrogen-bond network in the NaOX solution is represented by the Brownian oscillator model [Eq. (5)]. Here we observe that this spectral modulation results in an almost instantaneous broadening of the spectral holes observed in Fig. 3. Recently, infrared photon echo experiments[34] showed that the OH stretch vibration absorption band in water (HDO in D_2O) contains a component due to rapid spectral modulations with a half-width $\Delta_h = 60\ cm^{-1}$. The same result was found in spectral hole-burning studies of the OH stretch absorption band of HDO:D_2O[6]. Likely, the rapid fluctuations that are responsible for the broadening of the spectral holes observed for the NaOX solution are of the same nature as those causing the rapid echo decay and broad spectral holes observed for HDO:D_2O. This is in good agreement with our finding that $\Delta_{I,B}=65\ cm^{-1}$.

Since, apart from the absence of spectral diffusion, component I behaves similarly to HDO in D_2O, it is likely that Component I corresponds to HDO molecules that are hydrogen bonded to D_2O molecules [Fig. 2(a)]. Component II differs from component I in showing an extremely fast vibrational relaxation ($\sim$160 fs). The spectral response of this component (Table I) is quite similar to that of component I, which suggests that the OH groups forming component II have O–H$\cdots$O hydrogen bond lengths similar to those of component I. Therefore, the mechanism of vibrational relaxation of component II must be different from that of component I or that of water.[28] Component II is likely related to OH groups of HDO molecules that are hydrogen bonded to D_2O molecules or OD^- ions that show proton or deuteron exchange, as in Fig. 2(b). According to *ab initio* molecular-dynamics simulations on the solvation of OD^- (Refs. 14 and 23), there are two solvation structures of the OD^- ion: (a) $D_9O_5^-$, which is relatively stable, and (b) $D_7O_4^-$, in which rapid deuteron hopping can occur. Structures (a) and (b) transform into each other typically every 2 to 3 ps. The deuteron transfers in structure (b) occur typically with intervals of 40–100 fs and require only very small changes of the positions of the individual oxygen atoms. At each deuteron transfer, a D_2O molecule is transformed into an OD^- ion (and vice versa), which effectively changes the position of the complex in the global hydrogen bond network, since with each hop, one D_2O molecule leaves the complex and another enters. Such a deuteron transfer has a strong impact on any excited OH vibrations in participating HDO molecules, as the hydrogen bonds inside the complex are shorter ($R = 2.6$ Å) than between the surrounding water molecules (2.8 Å). This change in hydrogen-bond length corresponds to large jumps in the OH frequency, and likely leads to rapid vibrational relaxation. This hypothesis can be tested by studying the vibrational relaxation of the OH stretch vibrations over a large frequency range. If proton or deuteron transfer directly leads to vibrational relaxation, meaning that $T_{II,1}$ is the deuteron exchange time, we should observe very similar relaxation time scales for component II at all frequencies. In Fig. 7, the result of an experiment is shown where we excited the NaOX solution at 3030 cm^{-1} and where we probed at 3100 cm^{-1}. At this frequency, there will be no HDO molecules belonging to component I and the absorbance is dominated by HDO molecules that form very strong

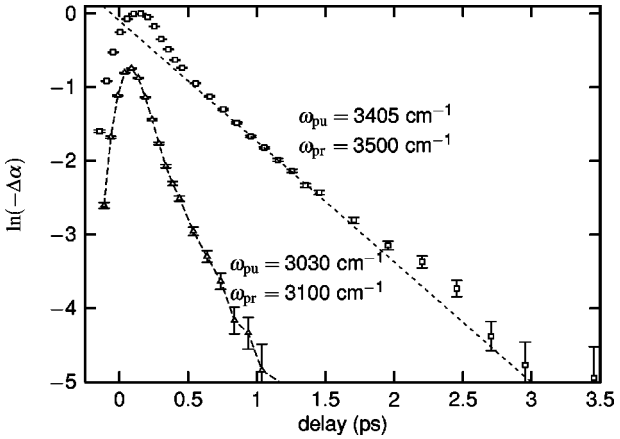

FIG. 7. Pump–probe transients with different pulse frequencies. Pumping at 3030 cm^{-1} results in a bleaching at 3100 cm^{-1} that has a decay rate comparable to that observed at much higher frequencies (Fig. 4). The line is a guide to the eye to indicate a purely exponential decay ($\tau = 0.61$ ps).

hydrogen bonded with OD^- ions. For this pump–probe combination a fast single-exponential decay is observed with a time constant of ~200 fs which is indeed very similar to the time constant observed for component II at much higher frequencies. This finding strongly supports the hypothesis that the vibrational lifetime of component II represents the characteristic time scale of the deuteron hopping.

The fact that the components I and II are so distinctly visible in the experimental data suggests that there is very little exchange between these components, even though there is one OX^- ion available for every 5.6 water molecules, of which 3 or 4 are needed to form the $HD_6O_4^-$ or $HD_8O_5^-$ complexes. It seems, therefore, that the deuteron exchange that causes the fast relaxation of the OH groups of component II is confined to certain regions in the hydrogen bond network.

V. CONCLUSIONS

With femtosecond two-color mid-infrared spectroscopy we found that persistent spectral holes can be burnt in the OH stretch absorbance spectrum of HDO molecules in a 10 M NaOD in D_2O solution. This shows that the hydrogen-bond network of this solution is far more rigid than that of pure liquid water, for which a rapid broadening of the spectral holes was observed ($\tau_c \approx 600$ fs).

The absorbance spectrum of the OH stretch vibration of the HDO molecules in a 10 M NaOD in D_2O consists of two components. Component I represents HDO molecules that are hydrogen bonded as $DO–H\cdots OD_2$ [Fig. 2(a)]. In comparison to the HDO molecules in pure liquid HDO:D_2O, the OH vibration of these molecules have a lower central frequency (3336 cm^{-1} instead of 3400 cm^{-1}), and they show a somewhat shorter vibrational lifetime (~600 fs (dependent on the OH frequency) instead of 740 fs). Component II consists of HDO molecules that are hydrogen bonded to D_2O molecules or OD^- ions that participate in proton transfers between HDO and OD^- or deuteron transfers between OD^- and D_2O [Fig. 2(b)]. The proton and deuteron transfers are accompanied by large jumps in frequency and lead to fast vibrational relaxation of component II. The time constant of this relaxation is ~160 fs, and likely represents the characteristic time scale of the deuteron hopping. This notion is supported by the observation that relaxation of component II is frequency independent, which means that OH groups that are strongly hydrogen bonded to OD^- ions show a very similar vibrational relaxation as OH groups that are weakly hydrogen bonded to D_2O molecules. The large difference in the vibrational relaxation time constants of components I and II also shows that these components exchange very slowly, which can be explained from the very rigid nature of the hydrogen-bond network.

ACKNOWLEDGMENTS

The work described in this paper is part of a collaborative research program of NIOK (Netherlands Graduate School of Catalysis Research) and FOM (Foundation for Fundamental Research on Matter), which is financially supported by NWO (Netherlands Organization for the Advancement of Research). These investigations were supported in part by The Netherlands Research Council for Chemical Sciences (NWO-CW).

[1] G. E. Walrafen, J. Chem. Phys. **44**, 1546 (1966).
[2] G. E. Walrafen, J. Chem. Phys. **52**, 4176 (1970).
[3] *Water: a comprehensive treatise*, edited by F. Franks (Plenum, New York, 1973), Vol. 3.
[4] M. F. Kropman and H. J. Bakker, Science **291**, 2118 (2001).
[5] S. Woutersen and H. J. Bakker, Phys. Rev. Lett. **83**, 2077 (1999).
[6] G. M. Gale, G. Gallot, F. Hache, N. Lascoux, S. Bratos, and J.-C. Leicknam, Phys. Rev. Lett. **82**, 1068 (1999).
[7] A. Novak, Struct. Bonding (Berlin) **18**, 177 (1974).
[8] W. Mikenda, J. Mol. Struct. **147**, 1 (1986).
[9] H. D. Lutz, Struct. Bonding (Berlin) **69**, 97 (1988).
[10] H. D. Lutz, Struct. Bonding (Berlin) **82**, 85 (1995).
[11] M. Rozenberg, A. Loewenschuss, and Y. Marcus, Phys. Chem. Chem. Phys. **2**, 2699 (2000).
[12] P. A. Giguère, Rev. Chim. Miner. **20**, 588 (1983).
[13] D. Schioberg and G. Zundel, J. Chem. Soc., Faraday Trans. 2 **69**, 771 (1973).
[14] M. E. Tuckerman, K. Laasonen, M. Sprik, and M. Parrinello, J. Chem. Phys. **103**, 150 (1995).
[15] M. E. Tuckerman, D. Marx, M. L. Klein, and M. Parrinello, Science **275**, 817 (1997).
[16] A. Vegiri and S. V. Shevkunov, J. Chem. Phys. **113**, 8521 (2000).
[17] D. Wei, E. I. Proynov, A. Milet, and D. R. Salahub, J. Phys. Chem. A **104**, 2384 (2000).
[18] M. Moskovits and K. M. Michaelian, J. Am. Chem. Soc. **102**, 2209 (1980).
[19] R. Buchner, G. Hefter, P. M. May, and P. Sipos, J. Phys. Chem. A **103**, 11186 (1999).
[20] F. Bruni, M. A. Ricci, and A. K. Soper, J. Chem. Phys. **114**, 8056 (2001).
[21] J. R. Pliego and J. M. Riveros, J. Chem. Phys. **112**, 4045 (2000).
[22] C. Chaudhuri, Y. S. Wang, J. C. Jiang, J. C. Jiang, Y. T. Lee, H. C. Chang, and G. Niedner-Schatteburg, Mol. Phys. **99**, 1161 (2001).
[23] M. E. Tuckerman, K. Laasonen, M. Sprik, and M. Parrinello, J. Phys. Chem. **99**, 5749 (1995).
[24] H. K. Nienhuys, R. A. van Santen, and H. J. Bakker, J. Chem. Phys. **112**, 8487 (2000).
[25] H. J. Bakker and H. K. Nienhuys, Science **297**, 507 (2002).
[26] H. J. Bakker, H. K. Nienhuys, G. Gallot, N. L. N , G. M. Gale, J.-C. Leicknam, and S. Bratos, J. Chem. Phys. **116**, 2592 (2002).
[27] R. E. Miller, Science **240**, 447 (1988).
[28] H. K. Nienhuys, S. Woutersen, R. A. van Santen, and H. J. Bakker, J. Chem. Phys. **111**, 1494 (1999).
[29] S. Mukamel, *Principles of nonlinear optical spectroscopy* (Oxford University Press, Oxford, 1991).
[30] *Tables of molecular vibrational frequencies consolidated*, edited by T.

Shimanouchi (National Bureau of Standards, Washington, D.C., 1972), Vol. I.
[31] A. Staib and J. T. Hynes, Chem. Phys. Lett. **204**, 197 (1993).
[32] *CRC Handbook of Chemistry and Physics*, 75th ed., edited by D. R. Lide (CRC, Boca Raton, 1994).
[33] J. Jonas, T. DeFries, and D. J. Wilbur, J. Chem. Phys. **65**, 582 (1976).
[34] J. Stenger, D. Madsen, P. Hamm, E. T. J. Nibbering, and T. Elsaesser, Phys. Rev. Lett. **87**, 027401 (2001).